

Scientific paper

Growth of Silver Nanoparticles Using Polythiocyanatohydroquinone in Aqueous Solution

Valentina A. Litvin,^{1,*} Boris F. Minaev,^{1,2} Rostislav L. Galagan,¹
Glib V. Baryshnikov^{1,2} and Hans Ågren²

¹ Department of Chemistry, Bohdan Khmelnytsky National University, Cherkassy, 18031, Ukraine

² Division of Theoretical Chemistry and Biology, School of Biotechnology, KTH Royal Institute of Technology, Stockholm, 10691, Sweden.

* Corresponding author: E-mail: litvin_valentina@ukr.net

Received: 12-01-2018

Abstract

Motivated by evidence that silver nanoparticles have found numerous technological applications we have explored in this work utilization of polythiocyanatohydroquinone as a new efficient reducing and stabilizing agent for the preparation of such nanoparticles. The formation of silver nanoparticles has been confirmed by the UV–Vis spectroscopy, X-ray powder diffraction and by transmission electron microscopy. The potentiometric and spectroscopy kinetic measurements during the nanoparticles growth are also presented. Thermodynamic activation parameters for the silver nanoparticle formation have been determined from the reaction kinetic studies at variable temperatures. On the ground of observations using these techniques, a mechanism for silver nanoparticle growth has been proposed. The narrow size (20–40 nm) and spherical shape distribution of the fabricated nanoparticles together with the high stability of colloids for sedimentation provide a firm basis for applications of the polythiocyanatohydroquinone polymer as a reducing and stabilizing material for the metal nanoparticles preparation and storage.

Keywords: Silver nanoparticles; polythiocyanatohydroquinone; potentiometric study; spectrophotometric study; kinetics

1. Introduction

Silver nanoparticles (AgNPs) are of special interest because of their unique physicochemical properties, including optical, magnetic and electronic characteristics, catalytic activity and biological impact,^{1–3} which make these particles applicable in a variety of technological areas in medicine, agriculture, environment, and industry.^{4,5} The AgNPs have also a high potential as commercial nanomaterials in cosmetics and as effective antimicrobial agents.^{1,6}

There are several methods proposed for fabrication of AgNPs, including chemical and physical approaches.^{7–9} Among them, the chemical reduction of silver ions in the presence of a protecting agent, is the most common and useful approach. Special attention is often devoted to the choice of reducing and capping agents since the physicochemical properties of the AgNPs are strongly dependent on the incorporated capping agent species.^{10–12} Organic polymers are in this context of especial interest because they can perform a reduction function while simultane-

ously being adsorbed on the nanoparticles surfaces thereby stabilizing them.^{13–16}

In this report we present the first attempt to synthesize AgNPs by using polythiocyanatohydroquinone (PTHQ)¹⁷ as a reducing and stabilizing agent with the aim to form the small size and highly distributed AgNPs. We present here kinetic investigations in order to predict the mechanism of the Ag⁺-ions reduction by PTHQ.

2. Experimental

2.1. Materials

All reagents (analytical-grade) were used as received from Sigma-Aldrich. De-ionized water (18 MΩ/cm) from a Millipore Milli-Q water purification system was used to prepare all aqueous solutions. The synthesis of PTHQ has been described previously.¹⁷ Briefly, the PTHQ was synthesized by the three-stage synthesis. The 1,4-benzoquinone crystal was dissolved in the glacial acetic acid (GAA) and treated with the NH₄SCN salt in the GGA medium.

The forming benzene-1,4-diol and thiocyanogen at the same conditions produce next the *ortho*-substituted 2-thiocyanatobenzene-1,4-diol which polymerizes rapidly into the target PTHQ compound. The orange-brown PTHQ polymer was precipitated by water, filtered, washed and dried upon 80 °C.

2. 1. Preparation of silver nanoparticles using PTHQ

In a typical experiment, a 19.6 mg of PTHQ was dissolved in 1.1 ml 1M solution of NaOH and the volume was adjusted to 60 mL with distilled water. The flask with resulting mixed solution was placed in a thermostat water bath at 30 °C. Next, 3.0 mL 0.2 M AgNO₃ was added under vigorous stirring. The final concentrations in the mixture were 1.67 mM PTHQ, 18.3 mM NaOH, and 10 mM AgNO₃.

Characterization. UV-Visible spectra were recorded as a function of reaction time on Lambda 35 Perkin Elmer UV-Visible spectrophotometer in the range of 320–520 nm. Aliquots of silver colloid (0.2 mL) were diluted to 25 ml for the UV-Visible experiments. The X-ray powder diffraction (XRD) analyses were performed on a DRON-2 X-ray diffractometer (LOMO, Russia) with Fe K α radiation ($\lambda = 1.9360 \text{ \AA}$) at a scanning speed of 0.01°/s over the 2 θ range of 20–120°. Transmission electron microscopy (TEM) was carried out by using a JEOL microscope (JEM-200A, Japan) with the accelerating voltage 200 kV. Samples for TEM investigations were prepared by evaporation of products on the surface of carbon films. The TEM images were registered with the CE video camera. The size of the particle can be calculated by using the scale provided in the micrograph. Potentiometric study the process of Ag-NPs formation was carried out on ionomer EV-74 with electrode system containing a glass electrode of type ESL-63–07 and a silver electrode of type EVL-1M3. As a reference electrode was used silver-oxide half-cell. The FT-IR spectra of the samples were recorded on Perkin-Elmer spectrometer (SpectrumGX) with a resolution of 2 cm⁻¹ over a scan range 4000–500 cm⁻¹ using KBr pellet method.

Computational details. The structure of PTHQ active site in different oxidized forms has been optimized as oligomer at the density functional theory (DFT) level using the B3LYP^{18,19} hybrid functional and the 6–31G(d)²⁰ basis set. The edge vacancies within –(C=N)– chain of the PTHQ polymer have been terminated by methyl groups in the oligomer model. We have also calculated the IR spectra for the studied species. All vibration frequencies were found to be real, which indicates the global minimum finding on the potential energy hypersurface. For the correct estimation of ionization potential (IP) values the polarizable continuum model (PCM)²¹ with water as a solvent has been used in the optimization procedure. The final IP values have been evaluated using Koopmans approach as the energy of the highest occupied molecular

orbital (HOMO) with the opposite sign (IP = – $\epsilon(\text{HOMO})$). All the calculations have been carried out using the Gaussian- 16 program package.²²

3. Results and Discussion

Stable aqueous colloids of AgNPs were prepared by chemical reduction of Ag⁺ ions using the PTHQ in the presence of NaOH. Due to the presences of phenolic group in the PTHQ structure¹⁷ the former reduces the Ag⁺ ions to Ag⁰ atoms and are then adsorbed on the surface of the growing AgNPs. In the alkaline medium the chemisorbed PTHQ species and their partially oxidized products possess a large negative charge due to ionization of the hydroxyl and carboxyl groups. The repulsive forces prevent the aggregation of nanoparticles and provide stability of the colloidal system. The final colloids are stable and can be stored more the one year without aggregation.

X-ray diffraction (XRD) results. The formation of the nanocrystalline AgNPs has been confirmed by the XRD analysis (Figure 1). Strong peaks observed at 48.6°, 56.8°, 84.5°, 104.1° and 110.9°, corresponding to the (111), (200), (220), (311) and (222) Bragg's reflections that determine the face-centered-cubic (fcc) crystal structure of Ag-NPs. The broadening of the Bragg's peaks indicates the formation of Ag NPs. The XRD pattern thus shows that the

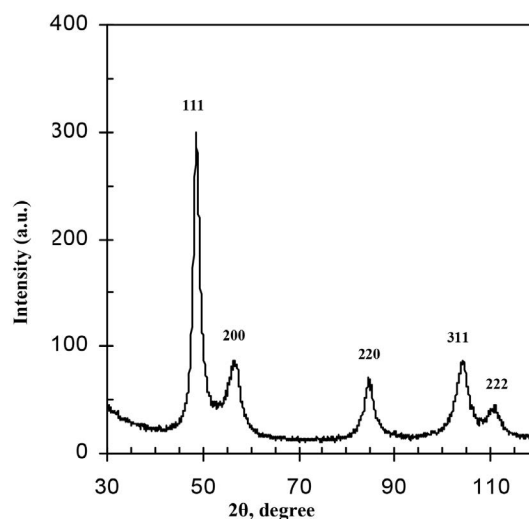


Fig. 1. XRD patterns of silver nanoparticles synthesized with PTHQ usage

Ag NPs formed by the reduction of Ag⁺ ions by PTHQ polymer are of the crystalline nature. The average size of the Ag nanoparticles has been calculated from the XRD line width using the Debye-Scherrer equation²³ and was found to be equal 20.8 nm.

Transmission electron microscopy (TEM) study. TEM was used to determine the size and shape of the nanoparticles. The TEM images of the PTHQ, prepared

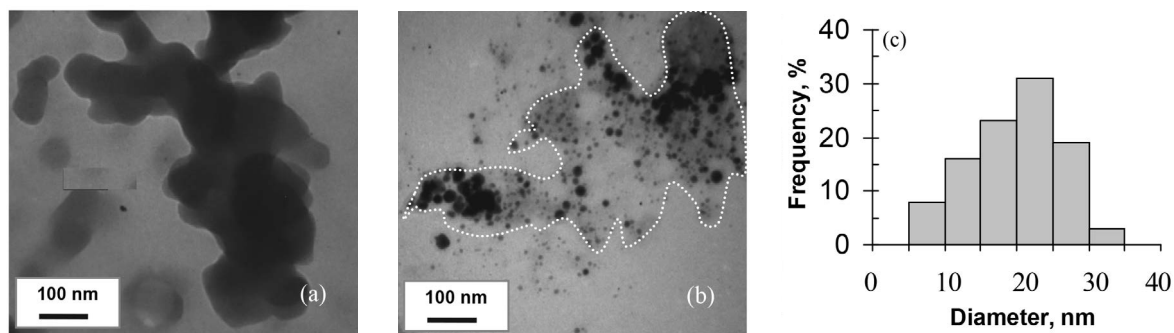


Fig. 2. The TEM images of PTHQ (a), AgNPs (b) and the corresponding size distribution histograms of AgNPs stabilized by PTHQ (c). The borders of the PTHQ globule are shown by the dotted line in part (b).

AgNPs are shown in the Fig. 2. TEM images show that they have spherical shape. A particle size distribution histogram determined from TEM is shown in Fig. 2c. The average AgNPs size is 19.8 nm. The particle sizes calculated from the XRD pattern have been found to vary within 5% of those obtained from TEM studies. The main difference of these hydrosols from similar nanosystems received with the use of other reducers, in particular the humic substances,¹⁵ is that the metal nanoparticles are fixed on the globule of the polymer.

Study of the silver nanoparticles formation by UV-Vis spectroscopy. The most popular method applied for the measurements of the kinetics of nanocluster formation in solution is UV-Visible spectroscopy since the sharp surface plasmon resonance band with maximum at 400 nm is a distinctive feature of the silver colloids.^{24,25} Evolution of the absorption spectrum of the silver colloidal solution during reduction of the Ag^+ ions by PTHQ at 30 °C is shown in Figure 3a. For the early stages of clusters formation, the broad absorption band near 480 nm appeared which indicates the formation of small Ag particles on the surface of the large Ag_2O particles. That position of this band absorption is the result in electronic interactions be-

tween the two types of materials because Ag_2O has semi-conducting properties. Research by the authors²⁶ has explained this fact by electron density transfer from the pure metal to the metal oxide nanoparticles when the small silver particles are formed on the surface of the n-type Ag_2O semiconductor. At longer reaction times, the absorption band shifts continuously to shorter wavelengths. The increase of absorption maximum intensity over the time is connected with continuation of the Ag^+ ions reduction process and with the increase of the number of the colloidal particles. The final surface plasmon resonance band has been observed at 400 nm (Figure 3a).

To investigate the reaction kinetics of the AgNPs formation, the absorbance at 400 nm has been plotted against the reaction time (Figure 3b). The visible absorbance of the product can be observed immediately after the mixing of the reagents and rises rapidly at the beginning of the reaction. Then absorbance reaches a plateau, which indicates the reaction completion (Figure 3b).

Proposed mechanism of silver nanoparticles formation. Evidently, at the initial stage of the Ag^+ cations reaction with the OH^- anions in the presence of PTHQ the formation of an Ag_2O microphase occurs. However, the

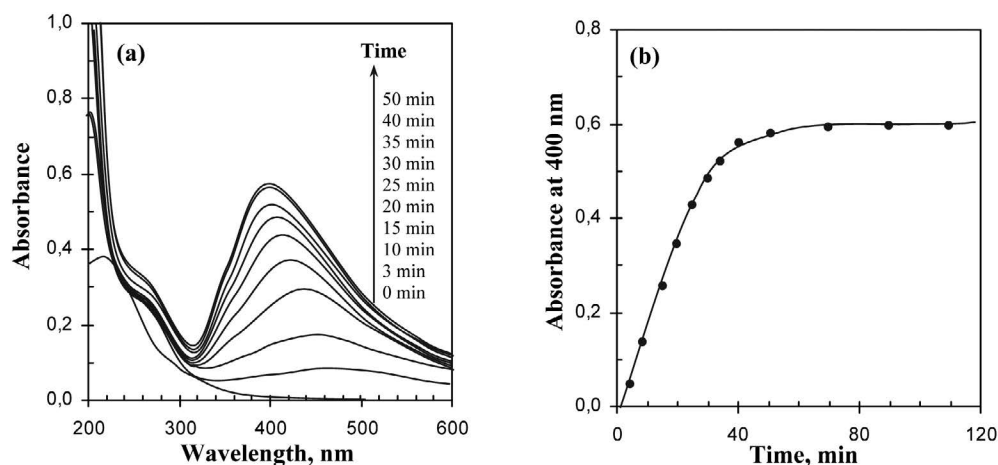


Fig. 3. The UV-Visible spectra of silver nanoparticles as a function of time (a); Absorbance at 400 nm versus time plot for the silver nanoparticles formation (b)

detection of Ag₂O microphase in similar systems by X-ray diffraction is extremely difficult, no matter how fast the separation of the precipitate from the solution is.²⁷ Huang et al.²⁶ have shown that it might be possible to capture some Ag₂O if the reaction was performed at a very low temperature (−45 °C).

The polymer chemisorbed on the Ag₂O particles in the alkaline environment has a negative charge due to ionization of the phenolic group, something that provides stabilization of nanoparticles. In the system “Ag₂O – organic reducer” few simultaneous processes can take place. The first of them is a dissolution of Ag₂O with the subsequent dissociation of AgOH:



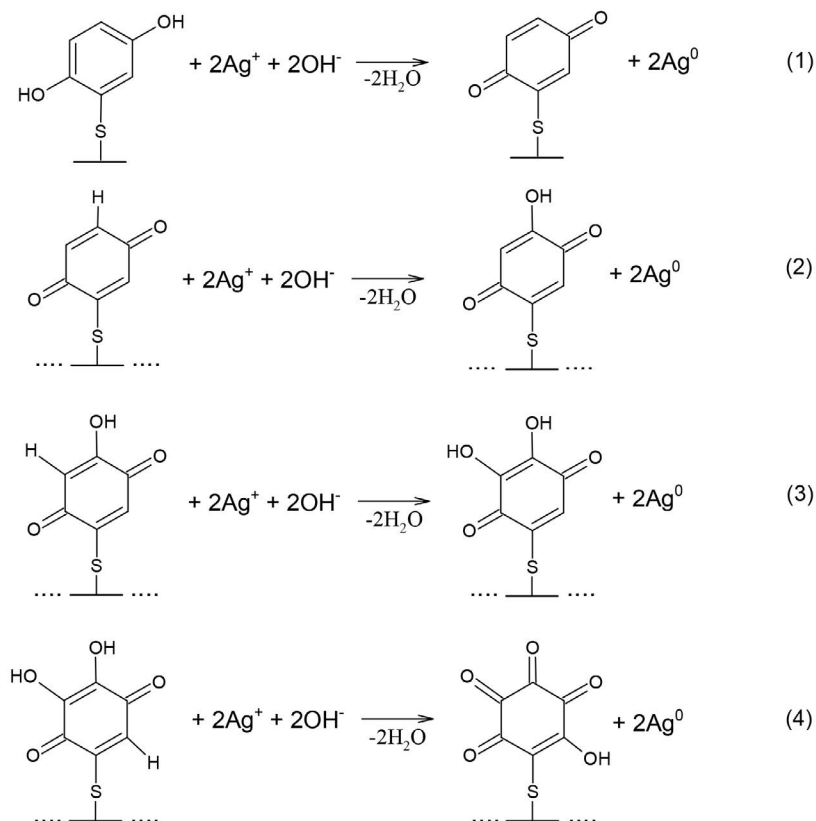
The equilibrium within the Ag₂O – H₂O system can be considered as a metallo-buffer for the Ag⁺ ions, and where the concentration of the latter shows a hyperbolic function of the OH[−] ion concentration. Thus, in water suspension of the Ag₂O species under intense stirring condition, the Ag⁺ ion concentration is expected to be constant and equal to 1.39 · 10^{−4} M (the solubility of Ag₂O is 1.95 · 10^{−8}).

At the same time, the other important process of the NPs growth includes interaction of PTHQ with Ag⁺ and

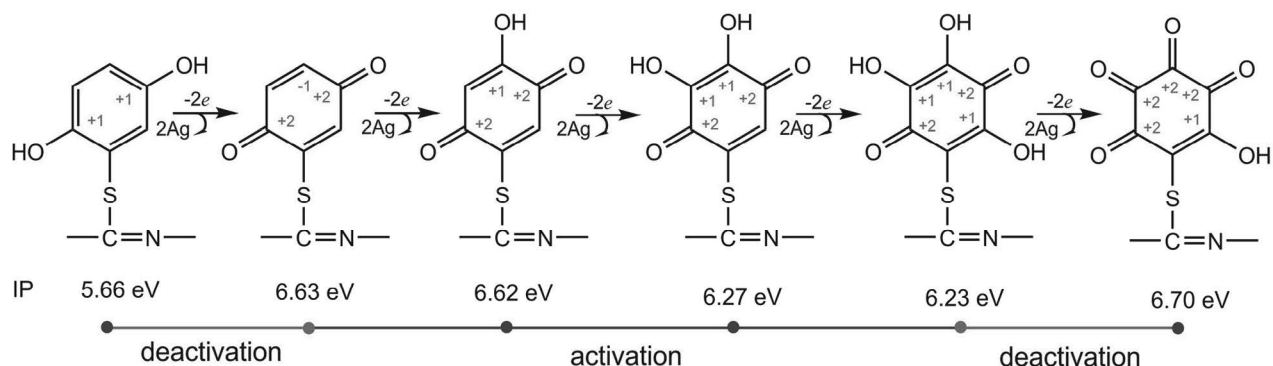
OH[−] ions, which results in the metal atom formation being aggregated into the nanoparticles. The major reducing groups in the structure of the PTHQ polymer are the phenolic groups, which are oxidized to the quinone structures. Thus, *in situ*-generated Ag₂O nanocrystallites act as heterogeneous nucleation centers. The reduction of Ag⁺ ions proceeds according to the following scheme:

The reduction reaction will proceed in the system until the whole Ag₂O microphase is dissolved or the reductive possibilities of the organic reducer will be exhausted. However, during the synthesis the molar ratio “Ag⁺: elementary link PTHQ” (*r*) did not exceed 6. If *r* > 6 a formation of a black deposit already in the course of the nanosystem synthesis was observed. Apparently, at excess of the ratio, the polymer will not have enough phenolic groups for delivery of a stabilizing charge to the complex particles [Ag@PTOH]^{x−} according to Eq. 4 (Scheme 1).

From this equation, it is clear, that the reductive ability of the aromatic core was practically exhausted, and that there is no possibility of formation of a sufficient amount of ionized hydroxyl groups for the maintenance of a negative charge of the complex. However, from the scheme 1 the possibility of a stable nanosystem formation at *r* = 8 follows, but the real ratio *r* is much lower because of the presence of the ditiocyanhydroquinone bridges in the PTHQ structure.



Scheme 1. Proposed mechanism for the reduction of Ag⁺ ions by PTHQ in alkaline media



Scheme 2. The reductive ability of PTHQ active site upon the gradual rising of silver cluster

In order to explain how the reductive ability of PTHQ changes with the AgNPs growing we have performed the quantum-chemical estimations for ionization potentials of the PTHQ active site in different oxidation states. As can be seen from Scheme 2 the ionization potential of the PTHQ active site increases strongly (5.66 vs. 6.63 eV) right after the first stage when two hydroxyl groups transform into carbonyl groups. Actually, this stage provides the deactivation of PTHQ for the next reduction activity. However, assuming the possible next oxidation steps of the quinone ring in Scheme 1 we have found that the corresponding ionization potential (IP) decreases gradually with the appearance of OH groups (6.63 eV for quinone ring vs. 6.23 eV for trihydroxyquinone moiety), i.e. the reductive ability of PTHQ increases with the addition of new OH groups. We consider these stages as the activation of PTHQ for reductive activity. Finally, the oxidation of trihydroxyquinone ring into the tetra-carbonyl form provides a complete deactivation of PTHQ active site due to its final IP increase and the complete electronic exhaustion.

Concluding shortly, we should note that these computational findings additionally approve the proposed mechanism (scheme 1) for the reduction of Ag^+ ions by PTHQ in alkaline media. Moreover, the tendency for the IP changes upon PTHQ oxidation sequence is in a good agreement with the experimental kinetic measurements data for the silver cation reduction.

Potentiometric study of the kinetics and mechanism of the silver nanoparticles formation. For real-time control of the Ag^+ ion reduction process, we have used a potentiometric method, as ion-selective electrodes (ISE) responds continuously and instantaneously to the changes of the silver ion concentration.^{28,29} The potentiometric method for studying the chemical reaction kinetic is based on measurements and interpretation of the time dependence of the redox potential for the indicator electrode reversible to the particles participating in the studied reaction. A use of this dependence in the kinetic studies is only possible if the rate of the establishment of the electrode equilibrium is higher than the rate of introduction of all others equilibriums in the system with the potential-deter-

mined particles. As the Ag^+/Ag system is one of the most prompt redox systems we can use the potentiometric method in our studies. Since the signal output of the ISE corresponds to the logarithm of the concentration of the solute ions, such a direct potentiometric control of the depleted metal ions provides additional information on the nanoparticle formation, which is not accessible by other techniques. In our work, we have used a simple silver electrode instead of ISE since the studied system does not contain any perturbing ions. The silver electrode is particularly useful for gaining information about the kinetic processes at later stages of the nanoparticle growth, in which case the solute ions become dilute and the concentration changes are much more easily discerned compared to other methods. The potentiometric curves of pAg as a function of time for the process of the AgNPs formation using PTHQ at different temperatures are shown in Fig. 4. The figure indicates a three-step growth process (*ab*; *bc* and *cd* site).

Let us consider the correspondence of different regions on the potentiometric curve (Fig. 4) to the kinetic stages of the process proposed in Scheme 1. The decrease of the pAg curve (*ab* site) indicates the balance displace-

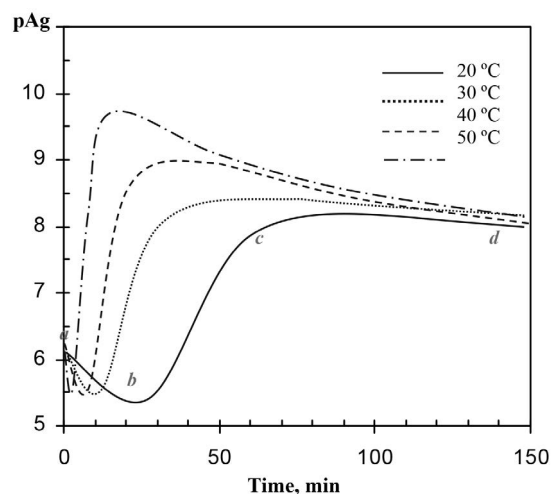


Fig. 4. The pAg potentiometric curves as a function of time for silver nanoparticles formation process at different temperatures

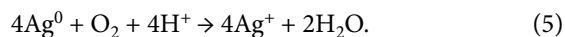
ment in Ag_2O dissociation as a result of a decrease in the concentration of the OH^- ions which are also the reagents of the given reaction.

As the reaction of silver ion reduction occurs on the surface of the Ag_2O particles (heterogeneous process), the rate of reaction does not depend on the Ag_2O concentration in solution. Thus, this stage is described by a zero-order kinetics in respect to Ag_2O and the rate constant (k_0) of the AgNPs formation at the initial stage can be found from the equation: $k_0 = dn(\text{Ag}_2\text{O})/dt$, where $n(\text{Ag}_2\text{O})$ – is an amount of the Ag_2O microphase (mole); t – time of the Ag_2O microphase existence in the system (s); k_0 – zero-order rate constant ($\text{mole} \cdot \text{s}^{-1}$).

At the point **b** of the pAg curve the whole Ag_2O microphase is dissolved and begins the growth of pAg values according to the linear law that specifies the first order reaction with respect to Ag^+ -ion. The rate constant at this stage can be found from the following equation: $k_1 = F/RT \cdot (\partial E/\partial t)_{T, \text{OH}^-, [\text{Ag}_n^0]}$, where k_1 – is the first-order rate constant (s^{-1}), F – is the Faraday constant ($9.65 \cdot 10^4$ coulomb/mole); R – the universal gas constant ($8.314 \text{ JK}^{-1}\text{mol}^{-1}$), T – temperature (K); $(\partial E/\partial t)_{T, \text{OH}^-, [\text{Ag}_n^0]}$ – the change of the equilibrium potential E of the Ag-electrode during the time t . The value of the derivative $(\partial E/\partial t)_{T, \text{OH}^-, [\text{Ag}_n^0]}$ was determined from the measurements of the slopes of the

linear parts of the pAg plots versus time (**bc** site, Fig. 5 A), taking into account that $E = 2.303 \cdot (RT/F) \cdot \Delta p\text{Ag}$.

At a point **c** the pAg curve passes through a maximum. Some decrease of the pAg values (**cd** site) corresponds to an increase in the concentration of the Ag^+ ions due to oxidation of the AgNPs by air oxygen^{30,31} according to the equation:



The process described by Eq. (5) was controlled by N_2 barbotation through the reaction solvent. In this case the pAg potentiometric curve after the point **c** in Fig. 4 does not go down. This is because the AgNPs are quite small and very reactive (the surface/volume ratio is great) in comparison with the massive silver metal.

On the ground of potentiometric curves it is possible to make a conclusion that the formation mechanism of the AgNPs with the use of PTHQ is similar to those mechanisms which use the synthetic humic substances;³⁰ in particular: 1) a fast formation of the Ag_2O microphase in the system after mixing of reagents; 2) reduction of silver ions on the surface of the Ag_2O particles according to the zero-order kinetics; 3) growth of AgNPs due to reduction of silver ions from solution on a surface of already generated

Table 1. Dependence of the rate constants at various temperatures for different stages of silver nanoparticles formation using PTHQ

Initial stage zero-order rate constants $k_0 \cdot 10^3$ ($\text{mole} \cdot \text{s}^{-1}$)				Later stage first-order rate constants $k_1 \cdot 10^3$ (s^{-1})			
293 K	303 K	313 K	323 K	293 K	303 K	313 K	323 K
0.25	0.60	0.92	1.20	1.62	3.83	5.64	7.50

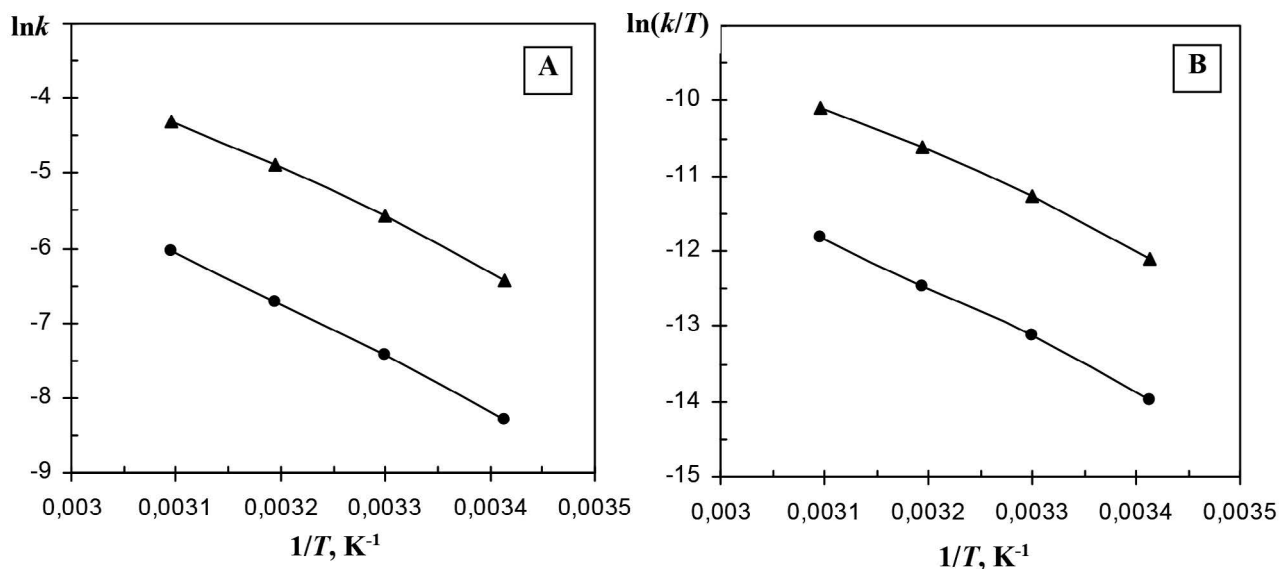


Fig. 5. The Arrhenius (A) and Eyring (B) plots of the silver nanoparticles formation for the initial (●) and later (▲) stages using the PTHQ reagent

nuclei of AgNPs according to the first order kinetics after the Ag₂O microphase dissolution.

The temperature influence on the reaction rate was also studied. Calculated values of the zero-order rate constant (k_0) for the initial stage of nanoparticles formation (before full dissolution of Ag₂O) and the first-order rate constants (k_1) at the later stages of the nanoparticle growth for different temperature are presented in Table 1. It is possible to observe that the reaction rate increases with temperature. No extra yield is obtained at higher temperature. The data suggest that the process can easily be promoted by the thermal activation mechanism.

Since the reduction of Ag⁺ ions occurs at the surface of Ag⁰ nuclei in the contact place of metal and silver oxide solid phases, the reaction rate does not depend on Ag₂O concentration in the solvent. Thus, the reaction rate constant of the Ag₂O depletion for the Ag NPs production at this initial stage is determined by the zero kinetic order according to equation $k_0 = dn(\text{Ag}_2\text{O})/dt$

Finally, from the Arrhenius Equation ($k = Ae^{-E_a/RT}$) and the Eyring Equation plots (Fig. 5), the activation parameters, e.g. the activation energy (E_a), the enthalpy (H^\ddagger) and entropy (S^\ddagger) of activation, were calculated.

The estimated values of these parameters for different stage of silver nanoparticle formation with the use of PTHQ as reducing and stabilizing agent are presented in Table 2.

The Ag₂O suspension is the source of the Ag⁺ ions at the initial stage. The rise of Ag⁺ ion concentration in Fig. 4 (*ab* site), being determined by the decrease in concentration of the OH⁻ ions working also as reagents in the reaction of Ag⁺ with PTHQ polymer, is an important prerequisite for the upcoming activation process. The latter includes reduction of the ions with the simultaneous growth of nanoparticles. The organic polymer is a reservoir of electrons for the reduction processes, which is rather complicated; the Ag⁺ ions at the first stage represent large rising concentration. The activation energy spent for electron transfer from PTHQ polymer (all averaged processes presented in Scheme 1) includes C-O and O-H bond cleavage with simultaneous ionization and subsequent electron attachment.

The similar processes occur at the later stage but in the limit of a decreased Ag⁺ ion concentration; the reaction strongly depends on this concentration (first order reaction). That is why the activation energies are quite similar for both stages (Table 2). The small difference can be connected with the fact that electronic resources are exhausted at the late step of the process.

4. Conclusions

A facile approach for the synthesis of stable aqueous colloids of silver nanoparticles (AgNPs) is described in the present work using the polythiocyanatohydroquinone (PTHQ) polymer as a reducing and stabilizing reagent in water. The AgNPs were characterized by different techniques such as UV-vis spectroscopy, X-ray diffraction and transmission electron microscopy. The TEM experiments indicate that these nanoparticles are formed with spherical shapes. The X-ray diffraction pattern shows a high purity and face centered cubic structure of the AgNPs. On the basis of various observations a three-step mechanism is proposed for the reduction of the silver ions by PTHQ: 1) a fast formation of the Ag₂O microphase in the system after mixing of reagents; 2) a reduction of the silver ions on the surface of the Ag₂O particles according to the zero-order kinetics; 3) a growth of AgNPs due to reduction of silver ions from a solution on the surface of already generated nuclear of AgNPs according to the first order kinetics after the Ag₂O microphase dissolution. The kinetic constants at various temperatures and for different stages were calculated and thermodynamic activation parameters were determined by variable temperature kinetic studies.

5. Acknowledgements

The quantum-chemical calculations were performed with computational resources provided by the High Performance Computing Center North (HPC2N) which is a Swedish national center for Scientific and Parallel Computing through the project “Multiphysics Modeling of Molecular Materials” SNIC 2016-34-43. This work was supported by the Ministry of Education and Science of Ukraine (Project No. 0117U003908).

The authors declare that they have no conflict of interest.

6. References

1. Yu. Krutyakov, A. A. Kudrinskiy, A. Yu. Olenin, G. V. Lisichkin, *Russ. Chem. Rev.*, **2008**, 77, 233–251.
DOI:10.1070/RC2008v077n03ABEH003751
2. A. Polman, H. A. Atwater, *Mater. Today*, **2005**, 8, 56.
DOI:10.1016/S1369-7021(04)00685-6

Table 2. Activation parameters for different stages of silver nanoparticles formation using PTHQ.

Activation energy E_a , kJ	Initial stage		Activation energy E_a , kJ	Later stage	
	ΔH^\ddagger , kJ mol ⁻¹	ΔS^\ddagger , J K ⁻¹ mol ⁻¹		ΔH^\ddagger , kJ mol ⁻¹	ΔS^\ddagger , J K ⁻¹ mol ⁻¹
58.90	56.34	-121.18	55.60	53.04	-116.74

3. K. Vasilev, V. R. Sah, R. V. Goreham, C. Ndi, R. D. Short, H. Griesser, *J. Nanotechnol.*, **2010**, *21*, 5102–5107.
4. S. Prabhu, E. Poulouse, *Int. Nano Lett.*, **2012**, *2*, 1–10.
DOI:10.1186/2228-5326-2-32
5. K. S. Lee, M. A. El-Sayed, *J. Phys. Chem. B*, **2006**, *110*, 19220–19225. DOI:10.1021/jp062536y
6. S. Kaviyaa, J. Santhanalakshmi, B. Viswanathan, J. Muthumary, K. Srinivasan, *Spectrochim. Acta A*, **2011**, *79*, 594–598.
DOI:10.1016/j.saa.2011.03.040
7. R. F. Elsupikhe, K. Shameli, M. B. Ahmad, N. A. Ibrahim, N. Zainudin, *Nanoscale Res. Lett.*, **2015**, *10*, 302.
DOI:10.1186/s11671-015-0916-1
8. J. Yang, H. Yin, J. Jia and Y. Wei, *Langmuir*, **2011**, *27*, 5047–5053. DOI:10.1021/la200013z
9. M. Harada, C. Kawasaki, K. Saijo, M. Demizu, Y. Kimura, *J. Colloid Interface Sci.*, **2010**, *343*, 537–545.
DOI:10.1016/j.jcis.2009.11.066
10. M. Manoth, K. Manzoor, M.K. Patra, P. Pandey, S.R. Vadera, N. Kumar, *Mater. Res. Bull.*, **2009**, *44*, 714–717.
DOI:10.1016/j.materresbull.2008.06.033
11. M. C. Rodriguez-Argüelles, C. Sieiro, R. Cao, L. Nasi, *J. Colloid Interface Sci.*, **2011**, *364*, 80–84.
DOI:10.1016/j.jcis.2011.08.006
12. M. M. Kemp, A. Kumar, S. Mousa, T.-J. Park, P. Ajayan, N. Kubotera, S. A. Mousa, R.J. Linhardt, *Biomacromolecules*, **2009**, *10*, 589–595. DOI:10.1021/bm801266t
13. V. A. Litvin, B. F. Minaev, G. V. Baryshnikov, *J. Mol. Struct.*, **2015**, *1086*, 25–33. DOI:10.1016/j.molstruc.2014.12.091
14. L. Quaroni, G. Chumanov, *J. Am. Chem. Soc.*, **1999**, *121*, 10642. DOI:10.1021/ja992088q
15. V. A. Litvin, B. F. Minaev, *Mater. Chem. Phys.*, **2014**, *144*, 168–178. DOI:10.1016/j.matchemphys.2013.12.039
16. V. A. Litvin, R.L. Galagan, B. F. Minaev, *Russ. J. Appl. Chem.*, **2012**, *85*, 296–302. DOI:10.1134/S1070427212020243
17. G. V. Baryshnikov, R. L. Galagan, L. P. Shepetun, V. A. Litvin, B. F. Minaev, *J. Mol. Struct.*, **2015**, *1096*, 15–20.
DOI:10.1016/j.molstruc.2015.04.040
18. D. Becke, *Phys. Rev. A*, **1988**, *38*, 3098–3100.
DOI:10.1103/PhysRevA.38.3098
19. C. Lee, W. Yang, R.G. Parr, *Phys. Rev. B*, **1988**, *37*, 785–789.
DOI:10.1103/PhysRevB.37.785
20. M. M. Francl, W. J. Pietro, W. J. Hehre, J. S. Binkley, M. S. Gordon, D. J. DeFrees, J. A. Pople, *J. Chem. Phys.*, **1982**, *77*, 3654–3665. DOI:10.1063/1.444267
21. S. Miertus, E. E. Scrocco, Tomasi, *J. Chem. Phys.*, **1981**, *55*, 117–129.
22. M. J. Frisch, G. W. Trucks, H. B. Schlegel, G. E. Scuseria, M. A. Robb, J. R. Cheeseman, G. Scalmani, V. Barone, G. A. Petersson, H. Nakatsuji, X. Li, M. Caricato, A. V. Marenich, J. Bloino, B. G. Janesko, R. Gomperts, B. Mennucci, H.P. Hratchian, J. V. Ortiz, A. F. Izmaylov, J. L. Sonnenberg, D. Williams-Young, F. Ding, F. Lipparini, F. Egidi, J. Goings, B. Peng, A. Petrone, T. Henderson, D. Ranasinghe, V. G. Zakrzewski, J. Gao, N. Rega, G. Zheng, W. Liang, M. Hada, M. Ehara, K. Toyota, R. Fukuda, J. Hasegawa, M. Ishida, T. Nakajima, Y. Honda, O. Kitao, H. Nakai, T. Vreven, K. Throssell, J. A. Montgomery, Jr., J. E. Peralta, F. Ogliaro, M. J. Bearpark, J. J. Heyd, E. N. Brothers, K. N. Kudin, V. N. Staroverov, T. A. Keith, R. Kobayashi, J. Normand, K. Raghavachari, A. P. Rendell, J. C. Burant, S. S. Iyengar, J. Tomasi, M. Cossi, J. M. Millam, M. Klene, C. Adamo, R. Cammi, J. W. Ochterski, R. L. Martin, K. Morokuma, O. Farkas, J. B. Foresman, D. J. Fox, Gaussian, Inc., Wallingford CT, 2016, Gaussian 16, Revision A.03.
23. C. Suryanarayana, M. Grantnorton X-Ray Diffraction: A Practical Approach, Plenum Publishing Corporation, New York, **1998**. DOI:10.1007/978-1-4899-0148-4
24. V. K. Vidhu, S. A. Aromal, D. Philip, *Spectrochim. Acta A*, **2011**, *83*, 392–397. DOI:10.1016/j.saa.2011.08.051
25. V. A. Litvin, B. F. Minaev, *Spectrochim. Acta A*, **2013**, *108*, 115–122. DOI:10.1016/j.saa.2013.01.049
26. Z.-Y. Huang, G. Mills, B. Hajek, *J. Phys. Chem.*, **1993**, *97*, 11542–11550. DOI:10.1021/j100146a031
27. K.-S. Chou, Yu.-C. Lu, H.-H. Lee, *Mater. Chem. Phys.*, **2005**, *94*, 429–433. DOI:10.1016/j.matchemphys.2005.05.029
28. T. C. Prathna, N. Chandrasekaran, A. M. Raichur, A. Mukherjee, *Colloids Surf. A*, **2011**, *377*, 212–216.
DOI:10.1016/j.colsurfa.2010.12.047
29. K. Y. Chumbimuni-Torres, E. Bakker, J. Wang, *Electroch. Commun.*, **2009**, *11*, 1964–1967.
DOI:10.1016/j.elecom.2009.08.029
30. V. A. Litvin, R. L. Galagan, B. F. Minaev, *Colloids Surf. A*, **2012**, *414*, 234–243. DOI:10.1016/j.colsurfa.2012.08.036
31. J. Liu, R. H. Hurt, *Environ. Sci. Technol.*, **2010**, *44*, 2169–2175.
DOI:10.1016/j.colsurfa.2012.08.036

Povzetek

Motivirani z dokazi, da imajo nanodelci srebra številne tehnološke aplikacije, smo v tem delu raziskali uporabo politiocianatohidrokinona kot novega učinkovitega redukcijskega in stabilizacijskega reagenta za pripravo takšnih nanodelcev. Nanodelce srebra smo karakterizirali z UV-Vis spektroskopijo, rentgensko praškovno difrakcijo in presevno elektronsko mikroskopijo (TEM). Predstavljene so tudi potenciometrične in spektrofotometrične kinetične meritve rasti nanodelcev srebra. Termodinamične aktivacijske parametre za tvorbo nanodelcev srebra smo določili iz reakcijskih kinetičnih študij pri različnih temperaturah. Predlagali smo mehanizem za nastanek nanodelcev srebra. Velikost (20–40 nm) in sferična porazdelitev nanodelcev skupaj z visoko stabilnostjo koloidov nam dajeta trdno osnovo za morebitno uporabo polimera kot redukcijskega in stabilizacijskega reagenta za pripravo in shranjevanje kovinskih nanodelcev.